REMOTE-SENSING THE WEATHER TO SUPPORT THE HONG KONG AIRPORT

K.C. Tsui, C.M. Cheng and B.Y. Lee

Hong Kong Observatory
134A Nathan Road, Kowloon, Hong Kong, China

ABSTRACT

The Hong Kong Observatory operates a number of remote-sensing equipment for monitoring the weather and issuing warnings in support of public and aviation weather services. This paper describes the functions and applications of these remote-sensing equipment. Plans to acquire additional equipment for enhancing the services in the next year or so will also be discussed.

1. Introduction

Remote-sensing equipment is widely used by weather services the world over in probing the atmosphere where weather systems form, develop and dissipate. The Hong Kong Observatory uses weather satellites, radars and wind profilers to monitor the weather in and around Hong Kong and to support the operations at the Hong Kong International Airport. In the following, various remote-sensing equipment implemented by the Observatory in recent years, their functions and applications are described.

2. Weather Satellites

The Observatory operates a ground reception system to receive satellite images broadcast from the Geostationary Meteorological Satellite-5 (GMS-5) of Japan. Located some 36,000 kilometres above the Equator at 140°E, GMS-5 closely follows the rotation of the earth, making it stationary relative to the globe. It captures cloud images in the Asian-Pacific region 24 hours a day (Figure 1). GMS-5 carries onboard a radiometer to measure upwelling radiation from the earth. Three types of images according to the wavelength of the received radiation are produced:

(a) Visible images: these images cover the wavelength range of 0.55-0.90μm and

record sunlight as reflected back from the earth. Clouds and snow have high reflectivity and show up in bright colours in the images. Land and sea without any cloud cover appear in dark grey. Compared with other image types, visible images offer the highest spatial resolution, providing reasonably fine details of clouds (Figure 2a). One limitation of visible images is that they are available only during daytime.

(b) Infrared images: Infrared images covering two wavelength ranges, i.e. 10.5-11.5μm (IR1 images) and 11.5-12.5μm (IR2 images), are received. The infrared radiation recorded on the images is a measure of temperature. Since temperature generally decreases with height, high clouds are colder and emit less infrared radiation than low clouds. Infrared images are therefore useful in differentiating between high and low clouds. Infrared images also allow estimation of tropical cyclone intensity. This makes them very useful in monitoring the intensity change of tropical cyclones. As a tropical cyclone intensifies, more high clouds develop near its centre, resulting in lower temperatures on the top of the tropical cyclone. Figure 2b depicts an infrared image of Typhoon Wukong in September 2000. Near the centre of Wukong, temperatures as low as –80° C were recorded, suggesting that the storm attained considerable strength. Infrared images are made available 24 hours a day, making them suitable for round-the-clock monitoring of the development of tropical cyclones.

(c) Water-vapour images: these images record radiation emitted from water vapour in the range of 6.5-7.0μm. Emissions from water vapour low in the atmosphere will not normally escape to space. If the upper atmosphere is moist, radiation emitted from water vapour there will be received by the radiometer and appear in brighter shades. When the upper atmosphere is dry, radiation originating from water vapour in the middle atmosphere will reach the radiometer and will appear in darker shades. Water-vapour images depict the atmospheric flow of the upper and middle atmospheres. Because of their availability 24 hours a day, they usefully supplement balloon-borne observations which are available only four times a day.

Apart from monitoring weather systems, satellite images can also be used to observe volcanic eruption. When there are no clouds covering the volcano, the ash erupting from the volcano is normally discernible on satellite images. When the volcano is obscured by clouds, an "IR2 minus IR1" image, representing differences in the received radiation between the two channels, offers an excellent tool in unravelling volcanic ash beneath clouds. The operating principle is that volcanic ash

and clouds exhibit different characteristics in the IR1 and IR2 infrared images. Figure 3 is an example of "IR2 minus IR1" image showing volcanic ash erupting from Mount Mayon in the Philippines in February 2000.

China launched a geostationary weather satellite called Fengyun-2B (FY-2B) in mid-2000. The satellite is currently under operational testing. Located above the Equator at 105°E, FY-2B has a good view of the Indian Ocean (Figure 1), making it suitable for monitoring weather systems approaching Hong Kong from the west. It also provides useful en-route weather information for long-haul flights westwards to places like Europe and Africa.

3. Doppler Weather Radars

While weather satellite images provide a global view of weather systems, weather radar enables close-up observation of weather systems likely to directly affect Hong Kong. Weather radar sends out pulses of microwave into the atmosphere to detect rain areas. When the microwave pulses hit the water droplets in a rain area, part of the energy of the microwave is reflected back to the radar (Figure 4). The round trip travel time of the microwave is used to calculate the distance to the rain area. The intensity of the rain area is estimated from the signal strength of the received microwave at the radar. The principle is that an intense rain area contains more water droplets, which reflect more microwave energy back to the radar, resulting in relatively high return signal strength.

Apart from detecting rain areas, Doppler radar can also measure the speed of movement of rain droplets relative to the radar. An example of such Doppler effect is the changes in the pitch of a train whistle when the train approaches and departs a station. The Doppler effect relevant to radar is illustrated in Figure 4. Doppler radar emits microwave at a frequency of f_0. When the water droplets in the rain area are moving relative to the radar, the frequency of the reflected microwave from the water droplets will be shifted to f_1. The shift in frequency, $f_1 - f_0$, has a direct relationship with the speed of water droplets relative to the radar and can be used to determine the radial velocity of the water droplets approaching or moving away from the radar.

The Observatory operates two S-band Doppler weather radars, one backing up the other, providing 24-hour surveillance of rain areas out to 500 kilometres from Hong Kong. They are located on the hilltops of Tai Mo Shan and Tate's Cairn,

separated by about 11 km (Figure 5). Their positions on hill-tops allow unobstructed view of the atmosphere around the radar sites. The radar at Tai Mo Shan operates at 2.82 GHz and has a narrow antenna beamwidth of 0.9° while the radar at Tate's Cairn operates at 2.92 GHz with an antenna beamwidth of 1.8°.

Radars are useful in determining the movement and development of rainstorms and tropical cyclones in the vicinity of Hong Kong. Some common radar products are: rainfall rate of rain areas at constant height above the ground (CAPPI – Constant Altitude Plan Position Indicator), vertical scan of a section across rain areas (RHI – Range Height Indicator), and maximum height of rain echoes (ECHO TOPS). By means of data processing technique, rain areas can be represented in a 3-dimensional view. Figure 6 shows a 3-dimensional image of Typhoon York which was moving towards Hong Kong at around 8 a.m. on 16 September 1999. From this image, the eye of York, i.e. the circular region with little rain, was clearly discernible. This allows close tracking of the storm.

Having two Doppler radars allows us to combine radial velocity information from the two radars to produce a wind pattern above Hong Kong. The usefulness of such dual Doppler winds in weather observation was demonstrated in the case of a Tropical Depression (TD) hitting Hong Kong in June this year. During the night of 18 June 2000, the TD formed over the water just to the south of Lantau Island. The TD headed north towards Hong Kong and made landfall near Tsuen Wan. Despite the fact that TDs are weakest in strength in the tropical cyclone hierarchy (other categories: tropical storm, severe tropical storm and typhoon, the latter being the strongest), the distinct circulation of the TD was well captured by the observed dual-Doppler winds of the TD when making landfall (Figure 7). Radars are very important tools for the forecasters to locate tropical cyclones, enabling issuance of tropical cyclone warnings to the general public and aviation users in a timely manner.

4. Terminal Doppler Weather Radar (TDWR)

Windshear is the variation of wind speed or wind direction in space. Turbulence also manifests itself as variation of wind speed and direction in space, but on a smaller length and time scale than those of windshear. Windshear and turbulence can be generated by topography or caused by severe weather such as thunderstorms. The most severe low-level windshear is microburst, caused by an intense down flow of air from an intense thunderstorm. The colder air aloft spreads out in all directions upon reaching the ground and produces strongly divergent winds. An aircraft flying

across the microburst will first encounter a strong head wind (hence increased lift), then a strong downdraught in the midst of the microburst, followed by a strong tail wind (hence decreased lift). Unless the pilot intervenes appropriately, the aircraft will deviate significantly from the intended flight path (Figure 8).

A Terminal Doppler Weather Radar (TDWR), operating at 5.625 GHz in the C-band, was installed at Tai Lam Chung (location shown in Figure 5) to detect windshear and turbulence near the aerodrome at Chek Lap Kok. The strategic location at Tai Lam Chung was chosen to gain a clear view of the runways, aircraft approach and departure areas. TDWR possesses all the typical functions of a Doppler weather radar in detecting the location, intensity and movement of rain areas near the airport. Unlike the Doppler radars at Tai Mo Shan and Tate's Cairn, however, the detection range of TDWR is shorter (around 90 km) but the high spatial resolution of TDWR is incomparable. This is attributed to its narrow antenna beamwidth of 0.5°. This unique feature, together with built-in data processing algorithms, allows the TDWR to depict in great details areas of convergent and divergent flows, making it possible to warn windshear and microburst caused by convective storms in the vicinity of the airport. An illustrative example is given by the passage of thunderstorms over Chek Lap Kok in the afternoon of 3 September 1999. Figure 9 shows the Doppler velocity pattern of the area of thunderstorms at 0737 UTC that day. Green and blue regions stand for velocities towards the radar while yellow and brown regions stand for velocities away from the radar. The "bandaid" shapes in the figure represent microburst areas detected by the TDWR. The grey rectangle outlines a region where opposing winds converged, and was caused by a gust front associated with downdraught from the intense thunderstorms.

Apart from windshear and microburst caused by convective storms, the TDWR is also capable of detecting terrain-induced windshear and turbulence in clear air under favourable conditions. On 18 March 1999, under a southerly airstream over the south China coastal area, a convergence zone (i.e. a region of converging winds) to the east of the airport was detected by the TDWR at about 0007 UTC (Figure 10). The TDWR did not observe any significant rain, but its Doppler wind pattern indicated that winds were deflected after passing through Yi Tung Shan (YTS), then turned southeasterly and converged with the prevailing southerly airflow at the wake of YTS. Aircraft flying through this convergence zone to the east of the airport would experience lifting force on the aircraft. In fact, an aircraft reported windshear of +30-35 kt at 0007 UTC, which represented an increase in head winds of 30-35 kt when the aircraft flew through the convergence zone. Such observation of

convergence aloft is not possible with ground based wind sensors (anemometers) alone.

5. Wind Profilers

A wind profiler operates very much like a radar and measures winds by means of Doppler effect. It transmits pulses of radio waves vertically upwards to the sky and measures the frequency of waves reflected by small eddies in the atmosphere. As these eddies move along with the wind, the shift in frequency from transmitted waves allows the wind velocity to be determined.

The Observatory operates three wind profilers at a frequency of 1.299 GHz in Hong Kong (locations indicated in Figure 5). Data collected by wind profilers are useful in monitoring the passage of tropical cyclones and low-level jets and in analysis of heavy rain.

Figure 11 shows the time series of wind profile measured at Sha Lo Wan during the passage of Maggie in June 1999. Maggie approached Hong Kong from the east, crossed Hong Kong from the northeast and passed to the south of Lantau. With a tropical cyclone on this track, winds near Sha Lo Wan would turn clockwise from the northwest to the east with time. Such change was indeed well captured by the wind profiler. An interesting feature in Figure 11 is that high winds aloft were observed to descend to lower altitudes as the storm closed in. This often provides the forecaster with a forewarning of increasing winds and deteriorating weather.

Another use of wind profilers is in detecting low-level jets. Low-level jet is signified by a region of high winds at low altitudes. Figure 12 shows a time cross-section of winds above Sha Lo Wan on 31 January 2000, clearly depicting a low level jet at around 1100 metres above the ground that morning. Aircraft moving across a low-level jet would experience a significant change in air speed, causing it to deviate from the intended flight path. Wind profiler enables the forecasters to warn pilots of windshear caused by a low-level jet.

6. Conclusion and Looking Ahead

Remote-sensing equipment comes in various types and functions. Over the last decade, the Hong Kong Observatory has in response to the emerging technology implemented a variety of remote sensing equipment to observe and monitor the

weather conditions to support the public and aviation weather services. The combination of weather satellites, Doppler radars and wind profilers allows the observation and detection of exciting weather phenomena and enables the forecaster to issue advance warnings to users. These were not possible 10 years ago.

There are several additional equipment to be acquired in the next couple of years. To back up reception of cloud images from GMS-5, the Observatory plans to implement a ground reception system to receive satellite cloud images from polar-orbiting satellites. These polar-orbiting satellites pass overhead only a couple of times each day, and this somewhat limits the number of satellite images available to the forecaster. However, compared with geostationary satellites, they circle around the earth on orbits much closer to the ground at altitudes of several hundred kilometres, acquiring cloud images of much higher resolution. This would allow greater details to be extracted from weather systems likely to affect Hong Kong, thus further improving weather warning services. The reception system is scheduled for implementation in mid-2001.

The Observatory also plans to install a radio acoustic sounding system (RASS) at Sha Lo Wan to operate side-by-side with the wind profiler there. The set-up will allow determination of temperatures aloft. Such temperature profile will be of considerable help in forecasting fog, haze and onset and cessation of sea breeze circulation. It will also ease the task of the forecaster in assessing the likelihood of thunderstorms and windshear for the short term.

Another plan of the Observatory is to implement a LIght Detection And Ranging (LIDAR) system at the airport in 2002. The LIDAR operates on a similar principle as the TDWR and uses infrared radiation to remotely sense the movement of atmospheric aerosols. It is expected to usefully complement the TDWR and will be able to discern areas of windshear better under clear air conditions. With the commissioning of the LIDAR system, we anticipate that the windshear and turbulence warning service at the Hong Kong airport will be further enhanced.

References

Ginn, E.W.L., S.C. Tai, and C.Y. Lam, 2000: "Dual-Doppler Observations of Severe Tropical Storm Maggie 1999", (submitted to *Weather and Forecasting*).

Hong Kong Observatory, 2000: "Tropical Cyclones in 1999".

Lau, S.Y., and S.T. Chan, 2000: "Case Study of Windshear caused by Low-level Jet", Hong Kong Observatory Technical Note No. 101.

Lee, O.S.M., and C.M. Shun, 1998: "Optimization of the Terminal Doppler Weather Radar for the Hong Kong International Airport", 2nd International Symposium on Electronics in Air Transport Industry (SEATI' 98), 18-19 November 1998, Hong Kong.

Yeung, K.K., 1998: "Use of Wind Profiler in Severe Weather Monitoring", *Meteorol. Zeitschrift*, N.F. 7, 326-331.

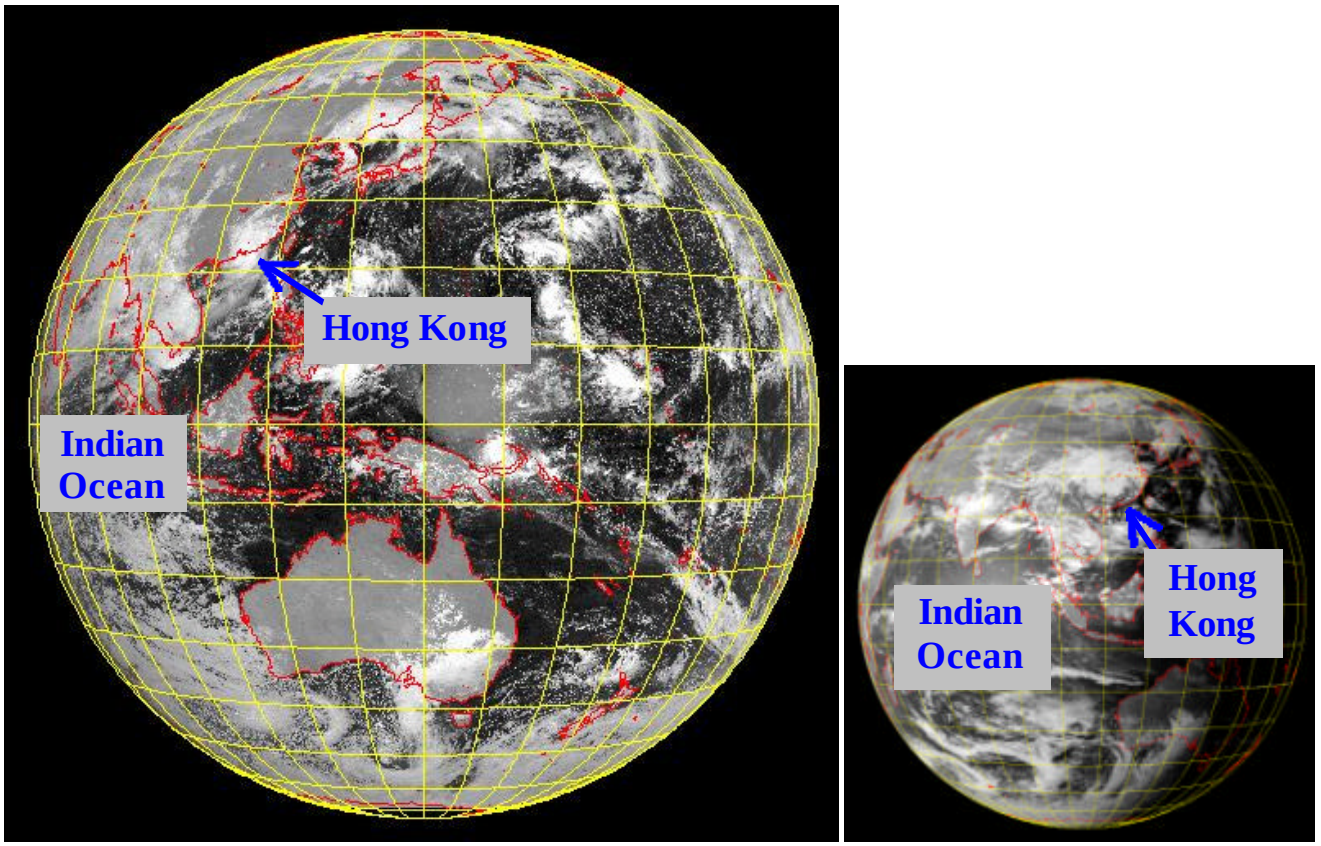

Figure 1 Visible satellite image at around 0130UTC on 1 September 2000 showing the geographical coverage of the GMS-5. (The image was originally captured by GMS-5 of Japan Meteorological Agency)

The inset is a visible image from FY-2B currently on trial (captured on 6 September 2000). The position of the satellite enables it to depict clearly weather systems over the Indian ocean. (The image was originally captured by FY-2B of China Meteorological Administration)

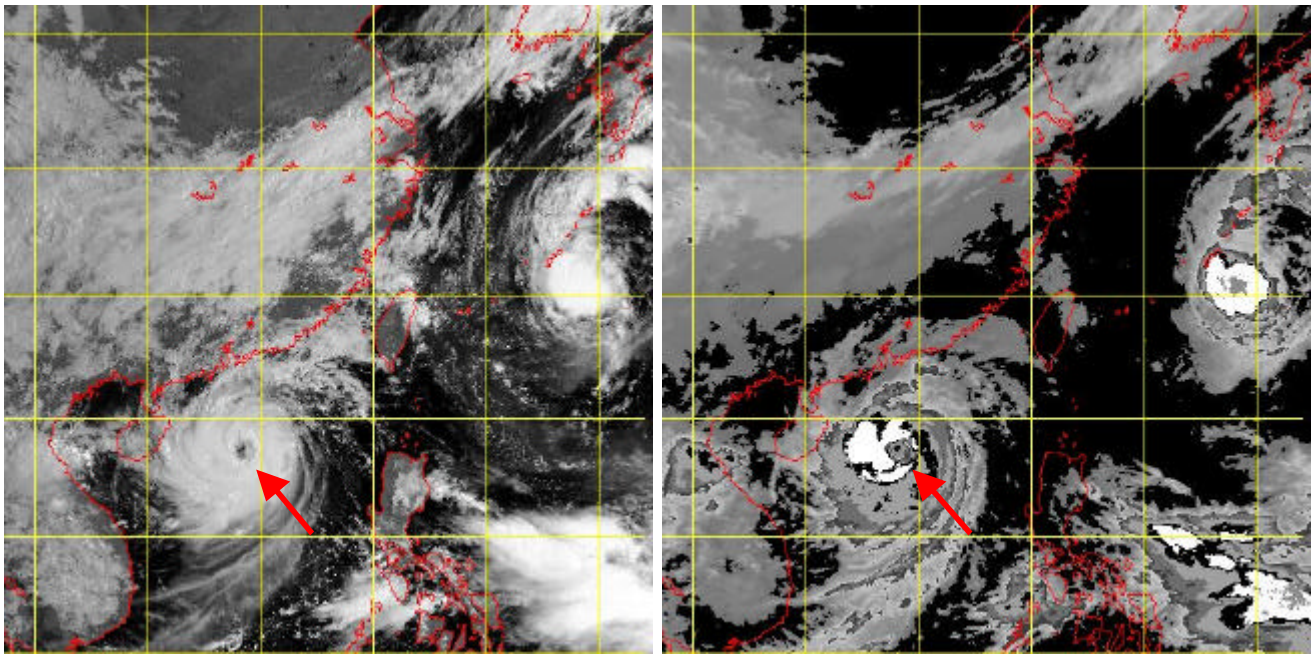

Figure 2 Satellite images captured at around 0030UTC on 8 September 2000 showing Typhoon Wukong over northern part of the South China Sea. The visible image on the left shows clearly the circular eye of Wukong. The infrared image on the right displays cloud temperatures in different shades of grey. The dark grey and white areas surrounding the eye of Wukong indicate temperatures as low as –80°C, suggesting that Wukong attained considerable strength. (The images were originally captured by GMS-5 of Japan Meteorological Agency)

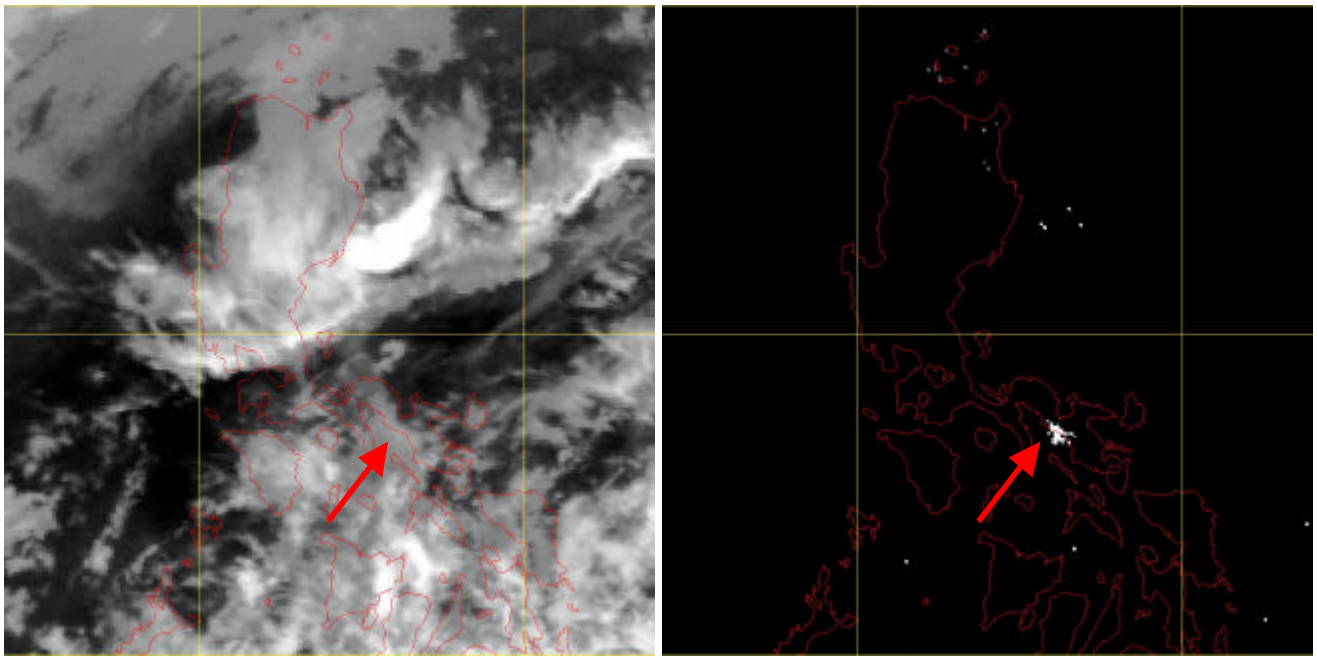

(a) (b)

Figure 3 (a) IR1 infrared satellite image at around 1130UTC on 29 February 2000. Volcanic ash erupting from Mount Mayon in the Philippines is obscured by clouds.
(b) "IR2 minus IR1" image showing ash clouds (indicated by an red arrow) erupting from Mount Mayon.
(The images were originally captured by GMS-5 of Japan Meteorological Agency)

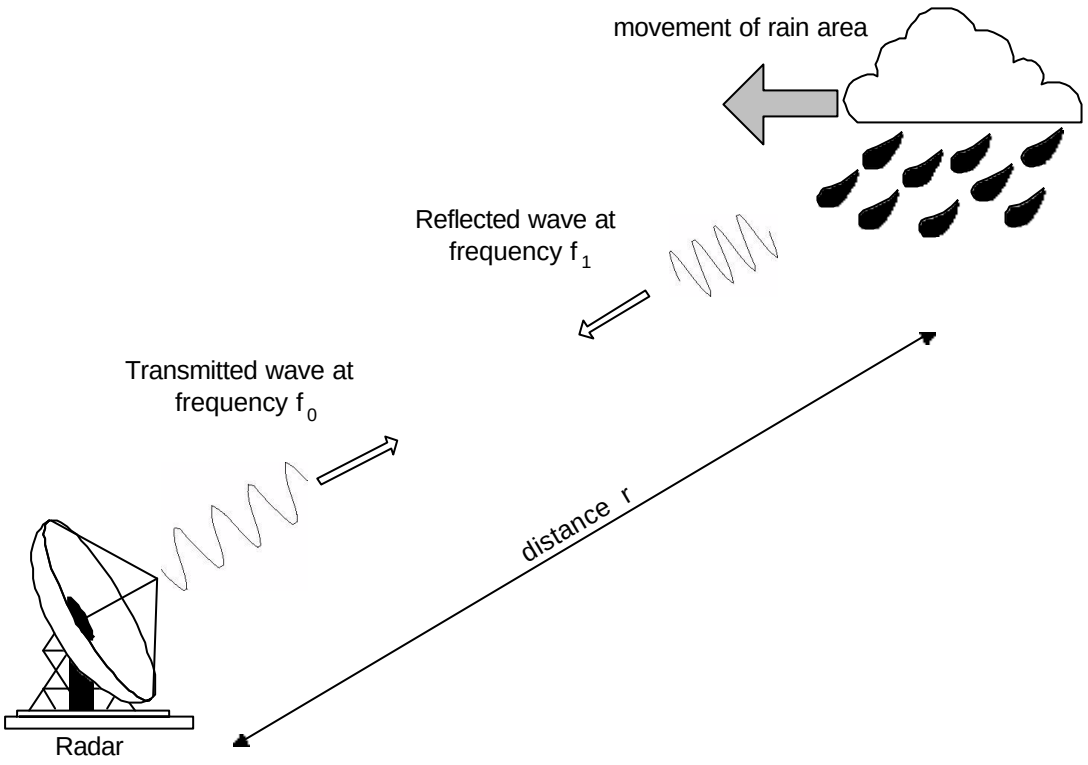

Figure 4 Schematic diagram showing the working principle of a Doppler weather radar in determining movement of rain areas. Radar emits pulses of microwave at a frequency of f_0 into the atmosphere. Upon hitting water droplets in a moving area of rain, the frequency of the reflected microwave is shifted to f_1. The reflected microwave is picked up by the radar for determination of approaching (or departing) velocity of water droplets in the rain area.

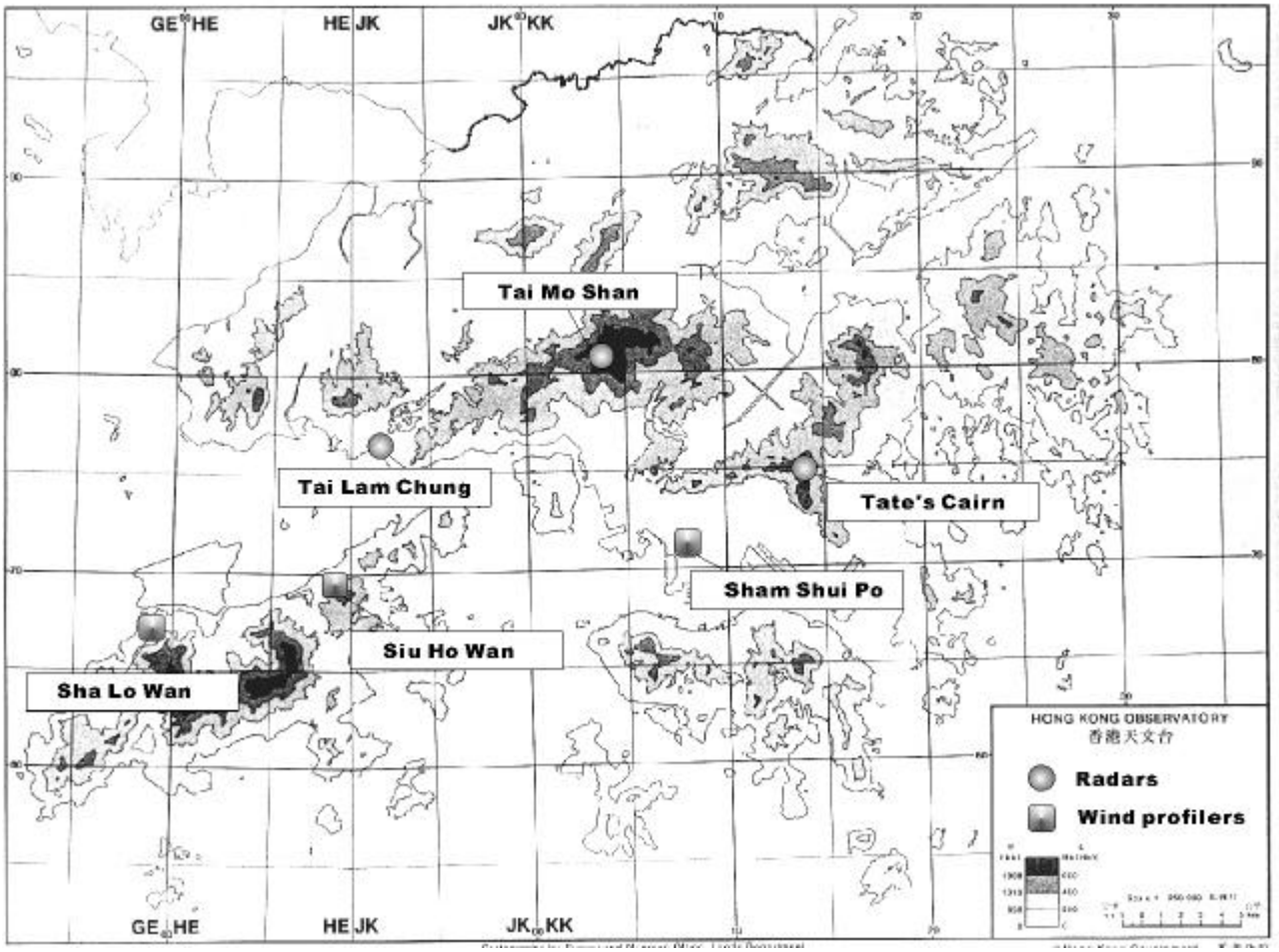

Figure 5 The locations of Doppler weather radars at Tai Mo Shan and Tate's Cairn, the Terminal Doppler Weather Radar at Tai Lam Chung, and wind profilers at Sham Shui Po, Sha Lo Wan and Siu Ho Wan.

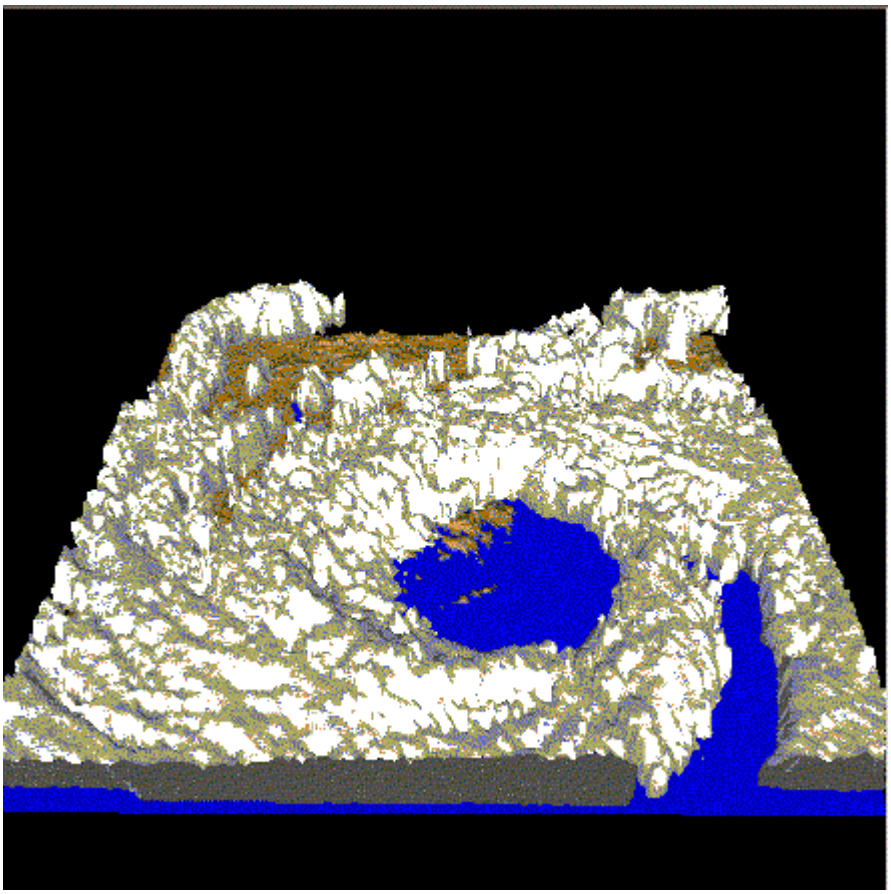

Figure 6 3-dimensional radar image of Typhoon York at around 8 a.m. on 16 September 1999. The relatively clear weather associated with the eye of York allows the southeastern part of Hong Kong to be discernible. The image reveals details of the structure of rainbands in the storm.

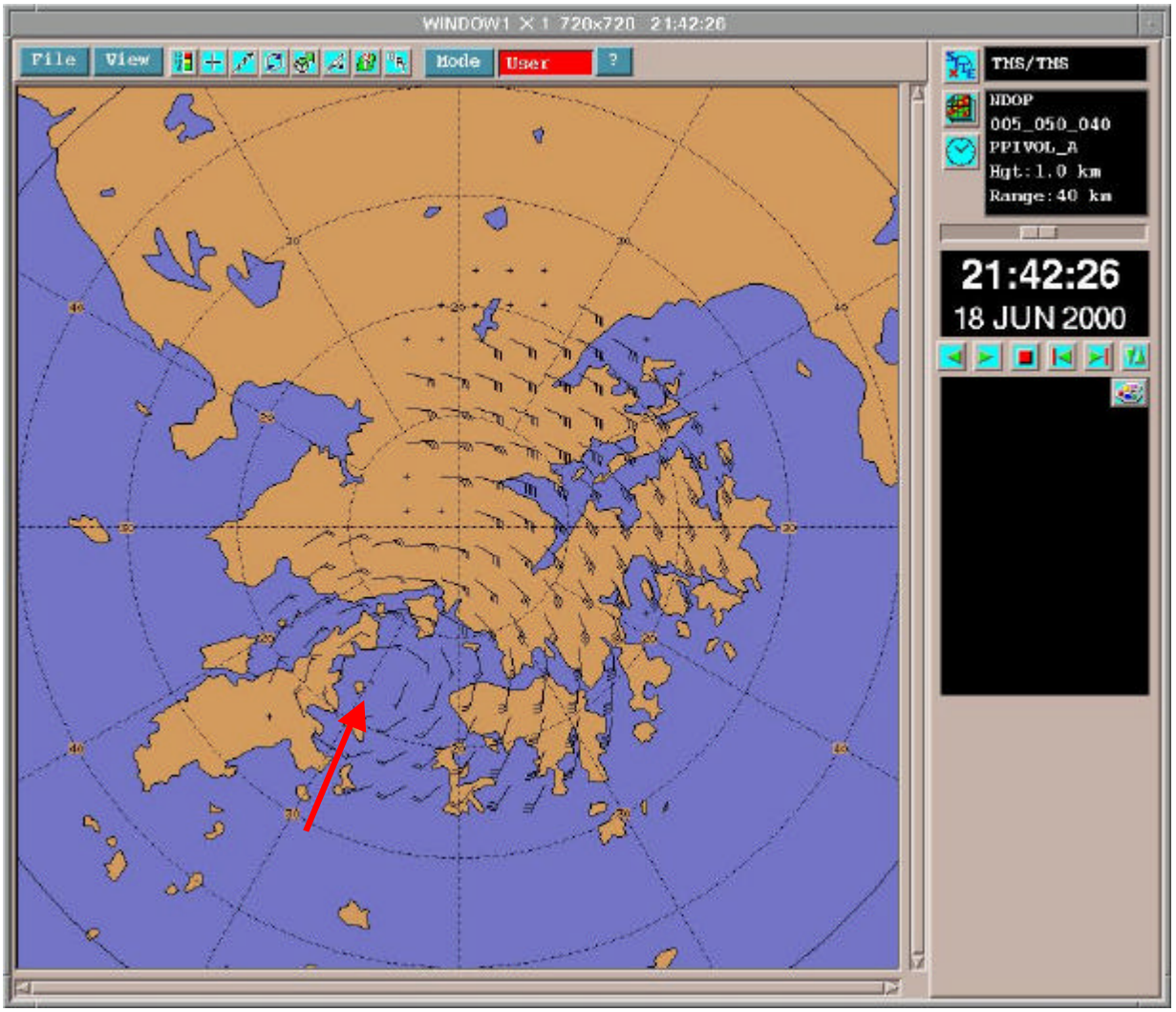

Figure 7 Dual-Doppler winds at 1-km height level for the tropical depression overhead Hong Kong at around 9:42p.m. on 18 June 2000. The wind pattern enables the circulation centre of the tropical depression to be easily determined (at that level).

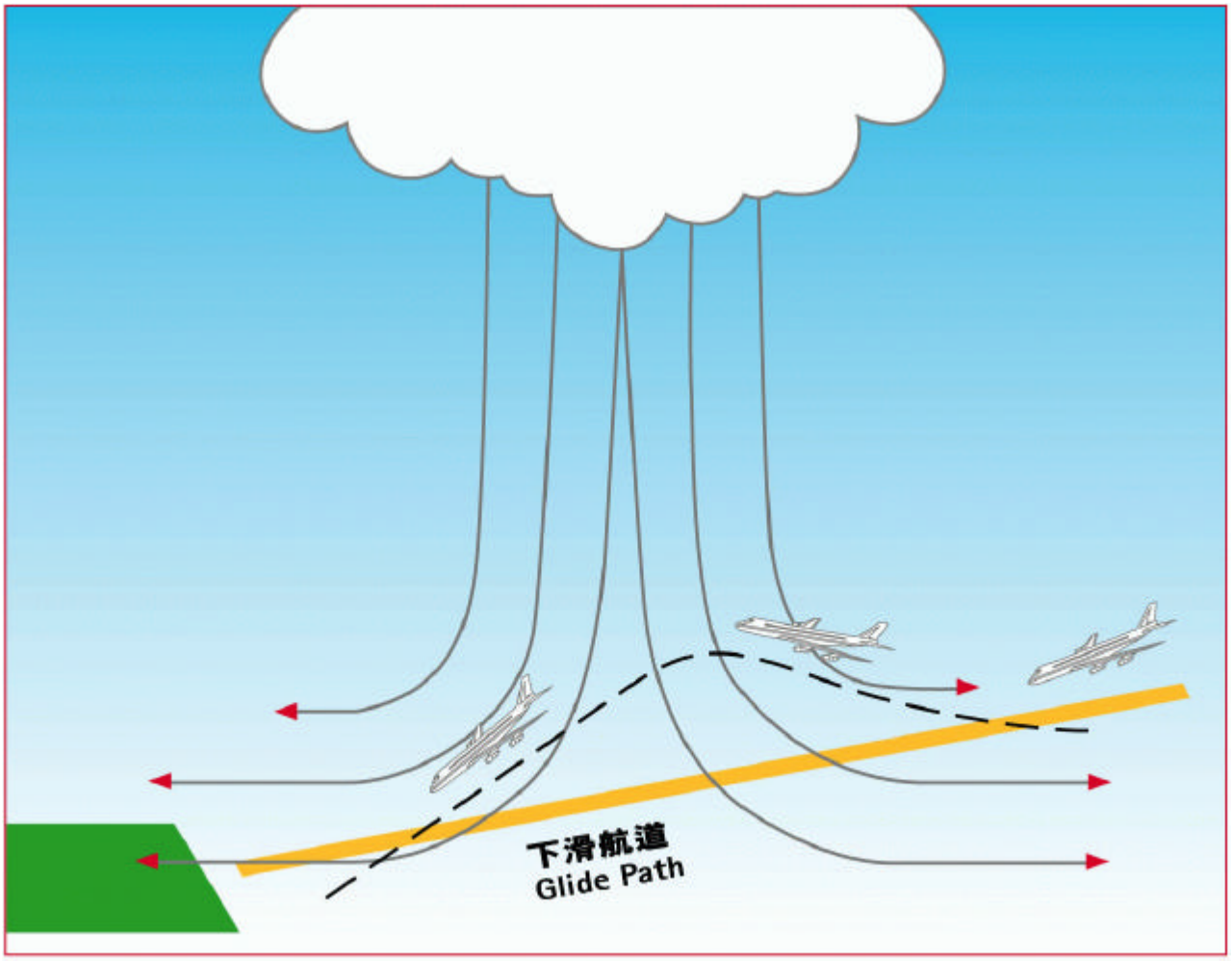

Figure 8 A conceptual diagram showing an aircraft flying across a microburst. The aircraft will first encounter a strong head wind producing lifting force. Thereafter it will experience sinking force as it continues its way to the region of strong downdraught at the core of the microburst.

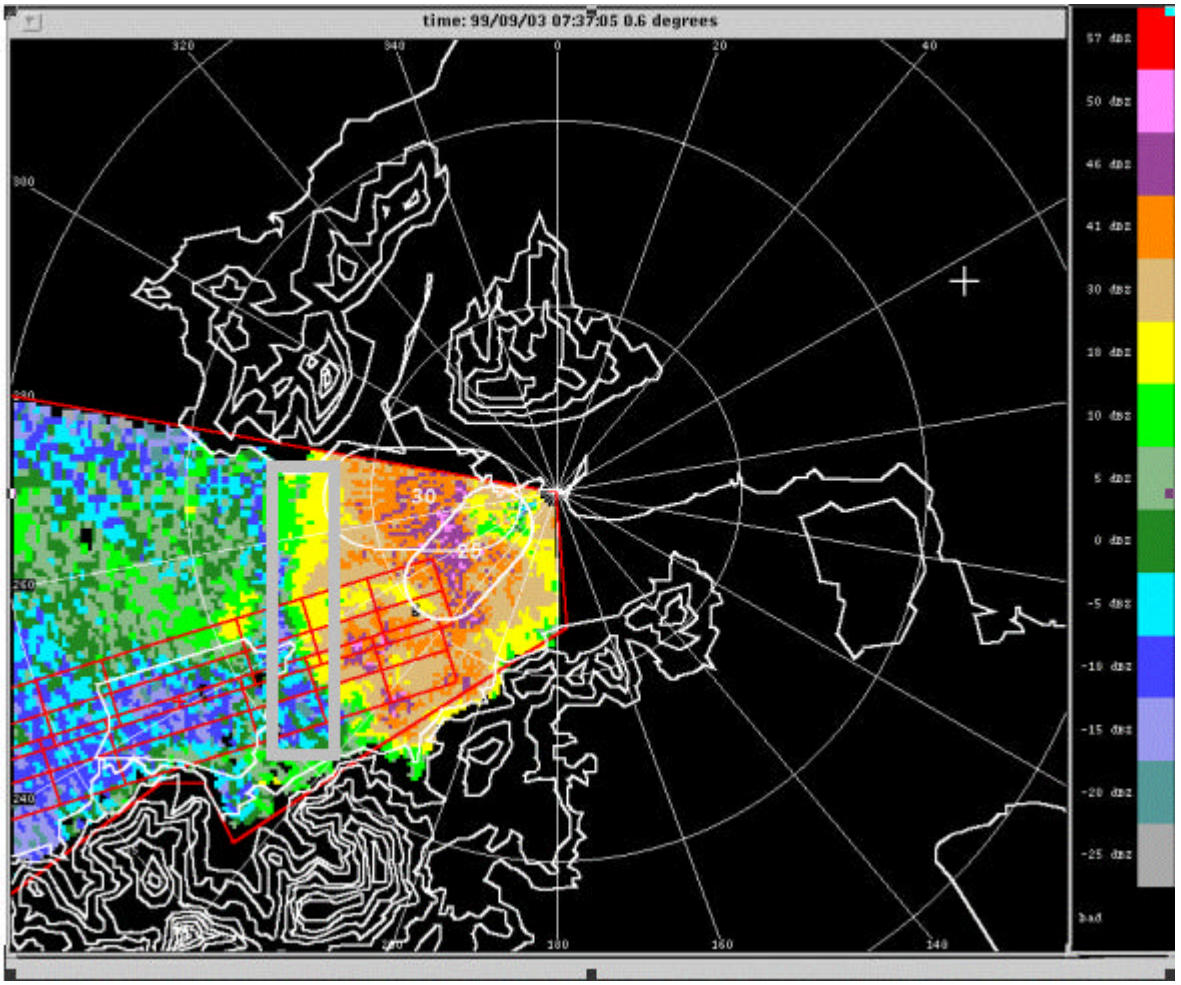

Figure 9 Doppler velocity at 0.6 degrees elevation from TDWR at 073705 UTC on 3 September 1999. The "bandaid" shapes represent microburst areas detected by the TDWR. The grey rectangle outlines a region of converging winds.

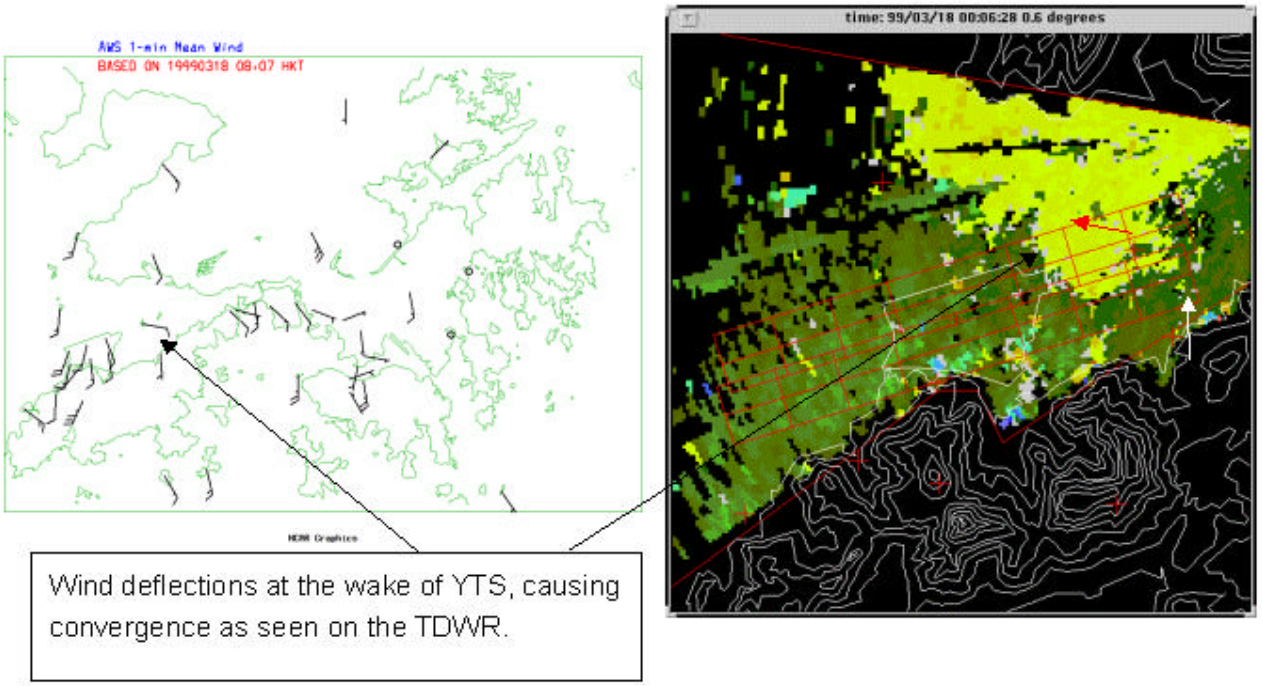

Figure 10 Terrain-induced windshear as observed by the automatic weather stations and the TDWR in the morning of 18 March 1999.

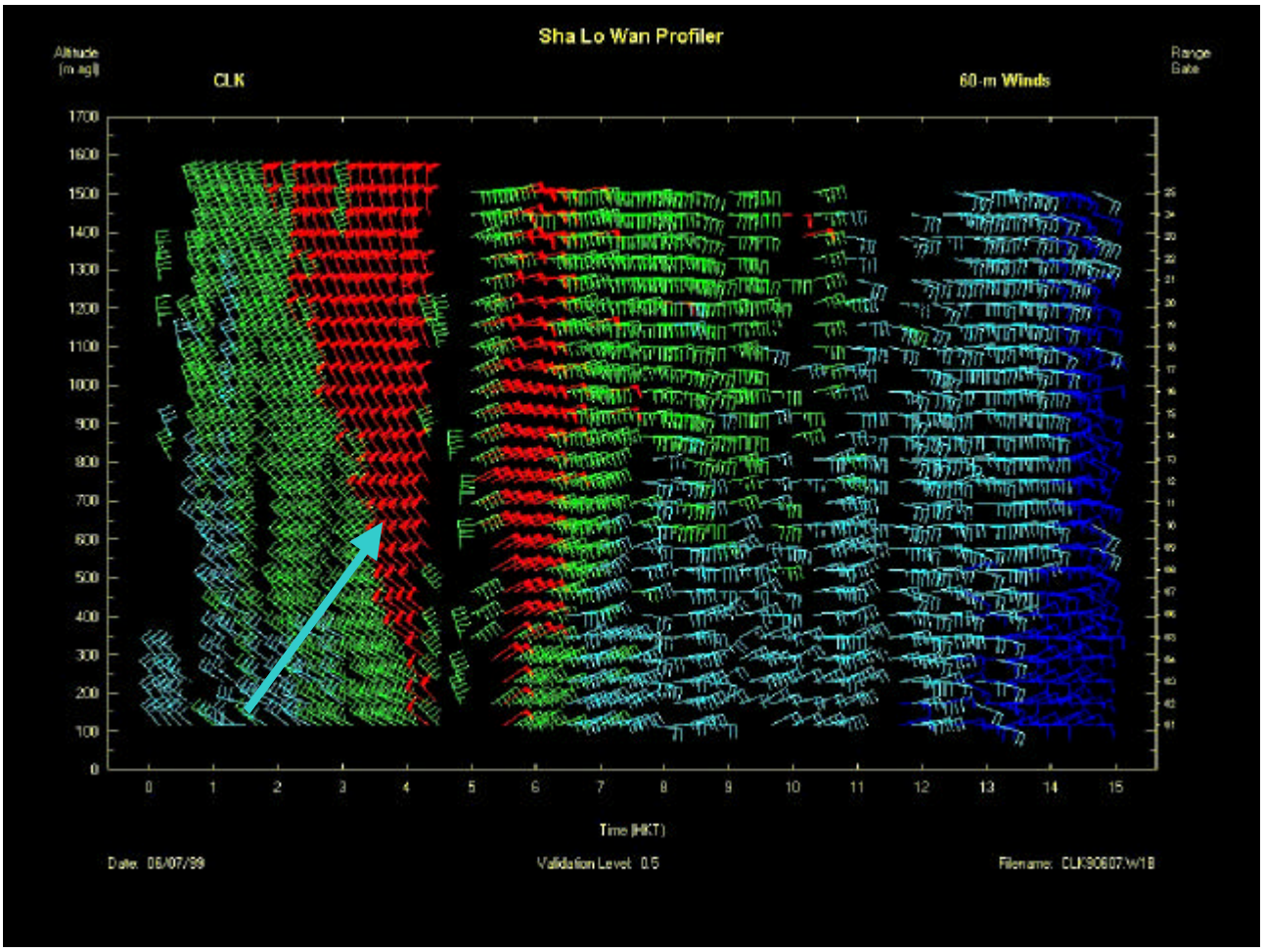

Figure 11 Time series of wind profile at Sha Lo Wan during passage of Maggie on 7 June 1999. It shows the descent with height of winds in excess of 50 knots (92 km/h) as Maggie moved across Hong Kong.

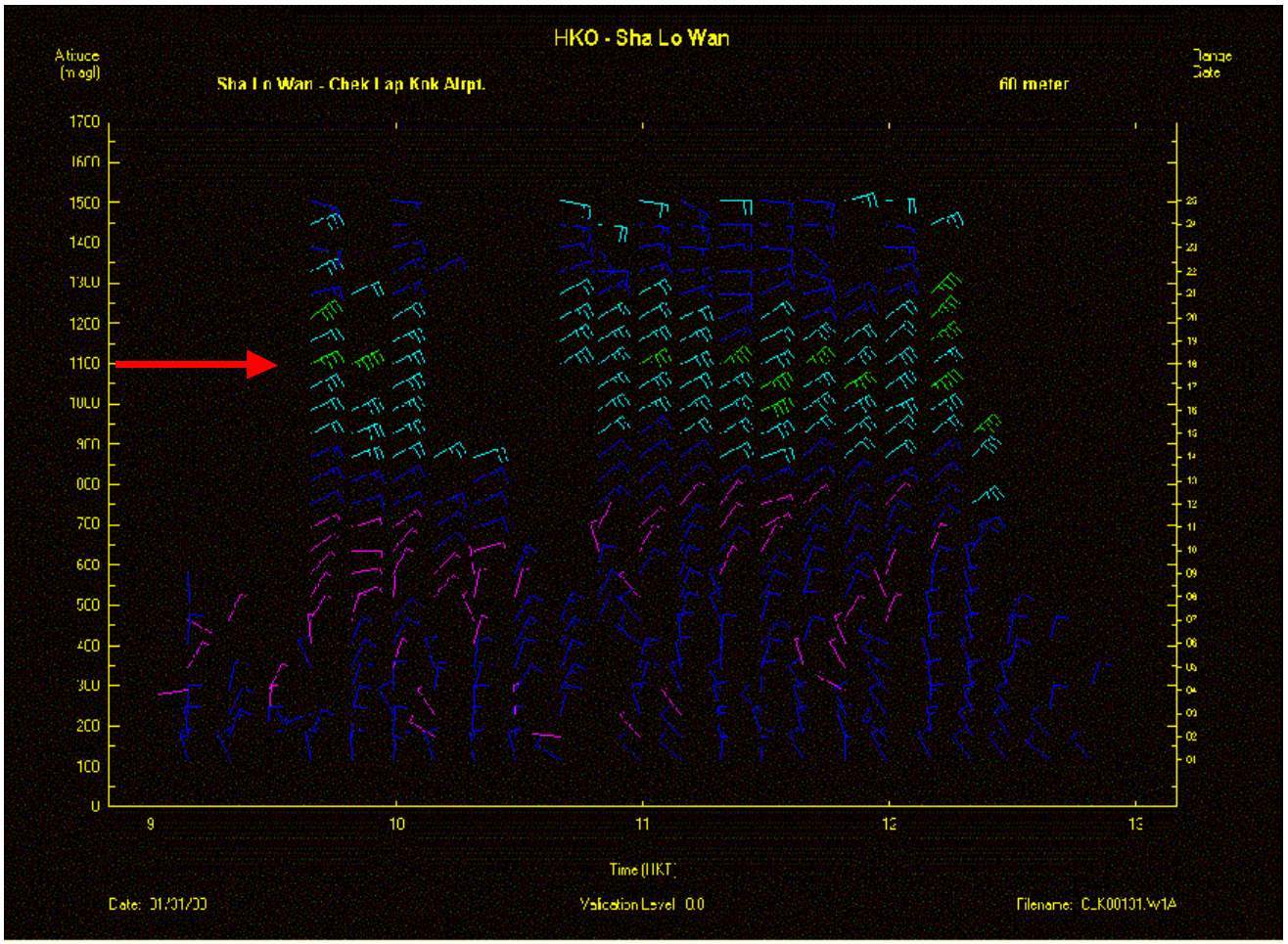

Figure 12 Time series of winds over Sha Lo Wan in the morning of 31 January 2000. A low level jet, signified by the region of strong to gale force winds at about 25-45 knots (47-83 km/h), is evident at an altitude of about 1100 m.